Instantaneous-shape sampling for calculation of the electromagnetic dipole strength in transitional nuclei

Zhang, S. Q.; Bentley, I.; Brant, Slobodan; Donau, F.; Frauendorf, S.; Kampfer, B.; Schwengner, R.; Wagner, A.

Instantaneous-shape sampling for calculation of the electromagnetic dipole strength in transitional nuclei

S. Q. Zhang,[1,*] I. Bentley,[1,2] S. Brant,[3] F. Dönau,[1] S. Frauendorf,[1,2] B. Kämpfer,[1] R. Schwengner,[1] and A. Wagner[1]

[1]*Institut für Strahlenphysik, Forschungszentrum Dresden-Rossendorf, D-01314 Dresden, Germany*
[2]*Department of Physics, University of Notre Dame, Notre Dame, Indiana 46556, USA*
[3]*Department of Physics, Faculty of Science, University of Zagreb, HR-10000 Zagreb, Croatia*

Electromagnetic dipole absorption cross sections of transitional nuclei with large-amplitude shape fluctuations are calculated in a microscopic way by introducing the concept of instantaneous-shape sampling, which is based on slow shape dynamics as compared with fast dipole vibrations. The dipole strength is calculated by means of the quasiparticle random-phase approximation (QRPA) for the instantaneous shapes, the probability of which is obtained by means of the interacting boson approximation. The calculations agree well with the experimental photoabsorption cross sections near the nucleon emission threshold, but they underestimate it at low energies. The cumulative cross sections for the region below the threshold are a factor of 2 too low.

Photonuclear processes, such as the absorption of a photon inducing the emission of a neutron or the emission of a photon after neutron absorption, are key elements in various astrophysical scenarios, e.g., supernovae explosions or γ-ray bursts, as well as in simulations for nuclear technology. For a quantitative description of the relevant nuclear reactions, one needs to know the photoabsorption cross section and the ree-mission probability, being determined by the dipole strength function. Direct measurements of the strength function in the relevant energy range (typically 6–10 MeV in medium-heavy nuclei) are not possible nowadays for most of the unstable nuclei passed in violent stellar events. Theoretical models that provide reliable predictions of the dipole strength function are therefore of utter importance. Aside from the astrophysical applications, understanding the mechanisms that determine the dipole strength function in this energy region is a challenge of its own to nuclear theory. The present communication proposes and tests a new approach, which we call instantaneous-shape sampling (ISS). It combines the microscopic quasiparticle random-phase approximation (QRPA) for dipole excitations with the phenomenological interacting boson approximation (IBA) for a dynamical treatment of the nuclear shape. ISS allows one to calculate the dipole strength function of the many transitional nuclei ranging between spherical and well-deformed shapes.

Traditionally, one employs phenomenological expressions for the dipole strength function [1], which are based on the classical model of a damped collective giant dipole resonance (GDR). The photoabsorption cross section σ_γ of the GDR is approximated by a Lorentzian curve [2,3], which may include corrections for nuclear deformation [3]. The damping width of the Lorentzian is treated as a parameter that is adjusted to the experiment. However, the available data have not yet allowed stringent tests of this extrapolation toward the low-energy tail

of the GDR [2]. Therefore microscopic approaches that treat at least a substantial part of the damping explicitly promise improved predictive power.

QRPA [4], the standard microscopic approach, takes into account the coupling of the collective dipole vibration to the one-quasiparticle excitations, which generates the Landau fragmentation. It also describes the splitting of the GDR caused by a static deformation of the mean field. However, both effects account for only a fraction of the observed width of the GDR. The remainder is generated by the coupling of the GDR to incoherent multiquasiparticle excitations (analog to the colli-sional damping of Fermi liquids) and to coherent collective excitations [4]. Quasiparticle-phonon coupling models, such as QPM [5,6], QTBA [7], and QRPA-PC [8], account for those additional couplings in spherical nuclei. However, principal problems arise in transitional nuclei.

We suggest an alternative approach. We explicitly describe the coupling of the dipole vibration to the one-quasiparticle excitations and to the low-energy collective quadrupole exci-tations, which represent the softest mode that couples most strongly to the dipole mode. The typical energies of the quadrupole excitations are $\hbar\omega_2 < 1$ MeV, i.e., about a factor of 10 less than the energies $\hbar\omega_1$ of the dipole excitations. Because the quadrupole motion is much slower than the dipole one, we use the adiabatic approximation: by means of QRPA, we calculate the dipole absorption cross section $\sigma_\gamma(E, \beta_n, \gamma_n)$ for a set of instantaneous deformation parameters $\{\beta_n, \gamma_n\}$ of the mean field. We determine the probability $P(\beta_n, \gamma_n)$ of each shape being present in the ground state and obtain the total cross section as the incoherent sum of the instantaneous ones,

$$\sigma_\gamma(E) = \sum_n P(\beta_n, \gamma_n) \sigma_\gamma(E, \beta_n, \gamma_n). \tag{1}$$

In other words, we assume that the quadrupole deformation does not change during the excitation of the nucleus by the absorbed photons, which sample the instantaneous shapes of the nucleus in the ground state. Accordingly, we call our method ISS-QRPA. Its applicability is further discussed below.

---

*On leave from School of Physics and State-Key Lab. Nucl. Phys. and Tech. Peking University, Beijing 100871, People's Republic of China.

TABLE I. IBA parameters ζ, χ, and e_B, and equilibrium deformation parameters β and γ calculated by means of the micro-macro method. In the case of shape coexistence, two sets are listed. Their respective proportion in the ground state is given in percentage.

^{A}X	ζ	χ	e_B	%	β	γ
^{88}Sr	0.0	−1.20	0.043	100	0.0	0°
^{90}Zr	0.0	−1.20	0.013	64	0.0	0°
	0.60	−0.31	0.040	36		
^{92}Mo	0.25	−1.32	0.040	100	0.0	0°
^{94}Mo	0.29	−1.20	0.064	100	0.02	60°
^{96}Mo	0.20	−1.32	0.069	100	0.10	60°
^{98}Mo	0.0	−1.20	0.053	60	0.18	37°
	0.59	−0.03	0.106	40		
^{100}Mo	0.0	−1.20	0.053	40	0.21	32°
	0.61	−0.10	0.106	60		

We adopt the QRPA version described in Ref. [9], combining a triaxial Woods-Saxon potential [10] with separable interactions. The pairing gaps are adjusted to the even-odd mass differences. Both the $E1$ and $M1$ responses are taken into account in calculating the total absorption cross section $\sigma_\gamma(E)$. For the $E1$ response, we use an isovector dipole-dipole interaction, with its strength being adjusted to the experimental GDR energy. The spurious center-of-mass motion is removed as described in Ref. [9]. For the $M1$ response, we combine a repulsive isovector spin-spin with an isoscalar quadrupole-quadrupole interaction [11]. The $\sigma_\gamma(E)$ is calculated by means of the strength function method with a resolution of 100 keV.

We describe the collective quadrupole mode by IBA-1 [12], which is known to well reproduce the development of energies and $E2$-transition probabilities from spherical to well-deformed nuclei through the transition region. We assume that the quadrupole operators in the IBA Hamiltonian and in the $E2$-transition operators are proportional to each other (the "extended consistent Q formalism"). Further we assume that the deformation of the charge distribution, derived from IBA, agrees with the one of the mean field, which is well founded. The IBA Hamiltonian and the $E2$-transition operators are given in Ref. [13]. The corresponding parameters ζ, χ, and e_B of the model are listed in Table I. We fix the boson number to $N_B = 10$, which turns out to be a sufficient flexible basis. The probability distribution $P(\beta_n, \gamma_n)$ is generated by means of the method suggested in Ref. [14]. We consider the two scalar operators

$$\hat{q}_2 = [Q^\chi \otimes Q^\chi]_0, \qquad (2)$$

$$\hat{q}_3 = [Q^\chi \otimes [Q^\chi \otimes Q^\chi]_2]_0, \qquad (3)$$

which are formed by angular momentum coupling from the IBA quadrupole operators Q^χ_μ. The commuting operators $\hat{q}_2$ and $\hat{q}_3$ are diagonalized in the space of states generated by coupling ten bosons to zero angular momentum. The resulting eigenvalues $q_{2,n}$ and $q_{3,n}$ and the eigenstates $|n\rangle$ are linked to the deformation parameters by

$$\beta_n^2 = \sqrt{5}\left(\frac{4\pi e_B}{3ZeR^2}\right)^2 q_{2,n}, \quad \cos 3\gamma_n = \sqrt{\frac{7}{2\sqrt{5}}}\frac{q_{3,n}}{(q_{2,n})^{3/2}}, \quad (4)$$

which assumes that the charge density and the mean field have the same deformation. The probabilities $P(\beta_n, \gamma_n) = |\langle 0_1^+|n\rangle|^2$ are the projections of the IBA ground state $|0_1^+\rangle$ on the set $|n\rangle$. In Ref. [15], Eq. (4) was used for the ground state *expectation values*, i.e., the mean values of the deformation parameters.

Some of the studied nuclei show shape coexistence; i.e., the low-lying 0_2^+ state and the 0_1^+ ground state are understood as mixtures of two different equilibrium shapes a and b with c_a^2 and $c_b^2 = 1 - c_a^2$ being the fractions of each shape in the ground state. In this case, two families of states originate from the collective motion about the two different equilibrium shapes, which we describe by two different IBA Hamiltonians. Using c_a^2 and c_b^2 and the experimental energies of the states 0_1^+ and 0_2^+, we calculate the energies of the pure states 0_a^+ and 0_b^+ and their interaction V. Assuming the same V for the states $2_1^+, 2_2^+, 4_1^+, 4_2^+$ (if observed), the energies and $B(E2)$ values of the pure states $2_a^+, 2_b^+, 4_a^+, 4_b^+$ are derived to which the IBA parameter sets a and b are fitted. We generate the probability distributions $P(\beta_{n,a}, \gamma_{n,a})$ and $P(\beta_{n,b}, \gamma_{n,b})$ for each of the two IBA Hamiltonians separately. The probabilities for all instantaneous shapes of the ground state are $c_\nu^2 P(\beta_{n,\nu}, \gamma_{n,\nu}), \nu = a, b$, and the sum in Eq. (1) is taken over all combinations $\{n, \nu\}$.

We applied the method to the nuclides ^{88}Sr, ^{90}Zr, and $^{92-100}$Mo, for which the combination of earlier (γ, n) measurements [1] with recent (γ, γ') experiments at the Forschungszentrum Rossendorf's superconducting electron linear accelerator ELBE [16–19] provided absorption cross sections $\sigma_\gamma(E)$ covering the whole energy range from the GDR down to a few MeV. The IBA parameters were obtained separately for each nuclide by fitting the energies and $B(E2)$ values of the lowest 0^+, 2^+, 4^+ states taken from the ENSDF data base [20] and from Refs. [21,22]. We set the boson number $N_B = 10$. Otherwise, we followed Refs. [21,22], from which we took the fractions c_a^2 and c_b^2 of the coexisting shapes in ^{90}Zr and ^{98,100}Mo. Figure 1 demonstrates that the resulting instantaneous shapes are widely distributed across the β-γ plane, which reflects the transitional nature of the considered nuclei. In the cases of shape coexistence, the two sets are distinguished by color.

In Ref. [23], the validity of ISS was studied for the case of the GDR coupled to quadrupole vibrations. ISS becomes a good approximation if $\eta = \frac{d\omega_1}{d\beta}\frac{\beta_0}{\omega_2} \gg 1$, where β_0 is the zero point amplitude of the quadrupole vibration. Typical values of $\eta \sim 5$ indicate that ISS is a reasonable approximation. We checked the quality of ISS in the region $E < 10$ MeV by comparing $\sigma_\gamma(E, \beta)$ calculated by QRPA for various deformation points β. In analyzing the shifts $\Delta\omega_1$ of the dominant QRPA peaks we find that the ratio $\frac{\Delta\omega_1}{\Delta\beta} \approx \frac{d\omega_1}{d\beta}$ scatters around a mean value of 10 MeV. Figure 1 indicates $\beta_0 = 0.1$–0.2. With $\hbar\omega_2 \approx$ 0.6–0.8 MeV, we find $\eta = 2$–5. This result and the observation that the peak structure of $\sigma_\gamma(E, \beta)$ changes in a chaotic way over intervals of $\Delta\beta = 0.05$ suggest that ISS, which incoherently combines the contributions from different shapes, is a reasonable approach. No low-lying octupole vibrations are observed in the considered nuclei, which justifies ignoring this mode in ISS. The coupling to excitations other than quadrupole becomes increasingly important with energy. We include it by folding with a Lorentzian of width $\Gamma = \alpha E^2$, which depends
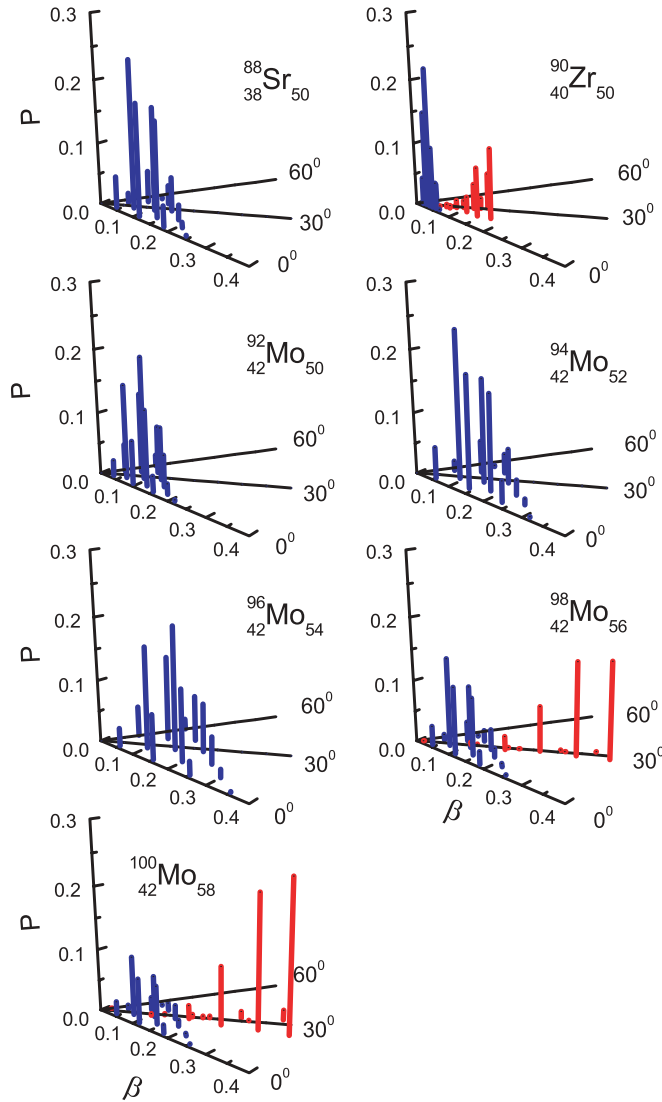
FIG. 1. (Color online) Probability distributions of the instantaneous nuclear shapes over the β-γ plane. Coexisting distributions are distinguished by their color.
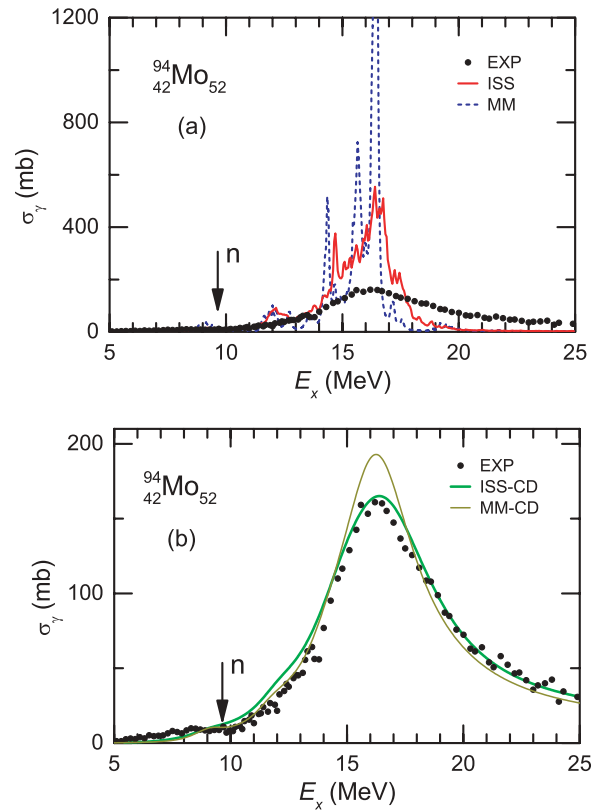

FIG. 2. (Color online) Photoabsorption cross sections of ^{94}Mo. (a) Cross sections as calculated in QRPA with a narrow width of 0.1 MeV. MM: for the equilibrium deformation; ISS: QRPA averaged over the probability distributions for the shapes in Fig. 1. (b) Corresponding cross sections MM-CD and ISS-CD, respectively, as obtained in QRPA by folding with an energy-dependent Lorentzian (see text). The experimental data (black dots) are from Ref. [17] in both figures.

on the photon energy E as expected for collisional damping [4]. The coefficient α is chosen to reproduce the experimental σ_γ at the maximum of the GDR, which gives $\alpha = 0.0105\,\mathrm{MeV}^{-1}$ for the neutron number $N = 50$ and $0.014\,\mathrm{MeV}^{-1}$ for $N > 50$.

Figures 2–4 compare the results with the experimental data. We include the QRPA results for the equilibrium deformations (labeled MM in the figures) listed in Tab. I, which were calculated by means of Strutinsky's shell correction method, referred to as the micro-macro (MM) method [9,11].

Let us first consider $^{94}_{42}$Mo$_{52}$ shown in Figs. 2(a), 2(b), and 3. It has a spherical equilibrium shape, but pronounced transitional character, which is demonstrated by the wide distribution of shapes in Fig. 1. The cross sections plotted in Fig. 2(a) are obtained from the QRPA strength function calculated with a narrow width of 100 keV, which singles out the Landau fragmentation. The spherical QRPA shows strong fluctuations of $\sigma_\gamma^{\mathrm{MM}}$, reflecting the degeneracy of the spherical single-particle levels. The substantial Landau

fragmentation shifts dipole strength into the threshold region. Sampling the different instantaneous shapes levels the strong spikes and shifts additional strength into the region below 14 MeV, such that $\sigma_\gamma^{\mathrm{ISS}}$ matches nicely with the experimental strength. Around the center of the GDR, the peak of $\sigma_\gamma^{\mathrm{ISS}}$ is broader and lower than the one of $\sigma_\gamma^{\mathrm{MM}}$; however, it is still too narrow and too high. This is because the QRPA with a narrow width neglects the collisional damping that becomes the dominant part of the resonance broadening in that region. In Fig. 2(b), the collisional damping is included by the above-mentioned energy-dependent width. The resulting cross section $\sigma_\gamma^{\mathrm{ISS-CD}}$ can reproduce the experimental one over the whole energy range. For the other nuclides, the overall agreement of $\sigma_\gamma^{\mathrm{ISS-CD}}(E)$ with the data is as good as in Fig. 2(b). The curve $\sigma_\gamma^{\mathrm{MM-CD}}$ includes Landau and collisional damping but excludes shape fluctuations. Since the peak height $\sigma_\gamma^{\mathrm{max}}$ is inversely proportional to the width Γ, one finds from

$$\frac{\sigma_\gamma^{\mathrm{max,ISS-CD}}}{\sigma_\gamma^{\mathrm{max,MM-CD}}} = \frac{160}{190} = \frac{\Gamma - \Gamma_{\mathrm{ISS}}}{\Gamma} \qquad (5)$$

that the shape fluctuations contribute $\Gamma_{\mathrm{ISS}} \approx 1\,\mathrm{MeV}$ to the total width of 5.7 MeV.
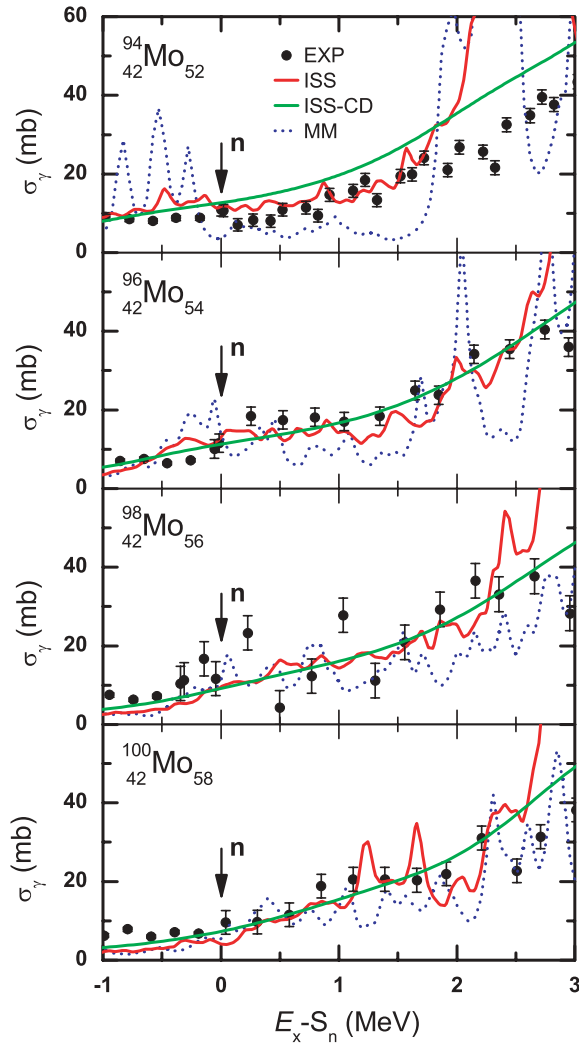
FIG. 3. (Color online) Same as Fig. 2, but for the energy range around the neutron emission threshold, where $S_n =$ 9.68, 9.15, 8.64, 8.29 MeV for $N =$ 52, 54, 56, 58, respectively. Data from Refs. [16,17].
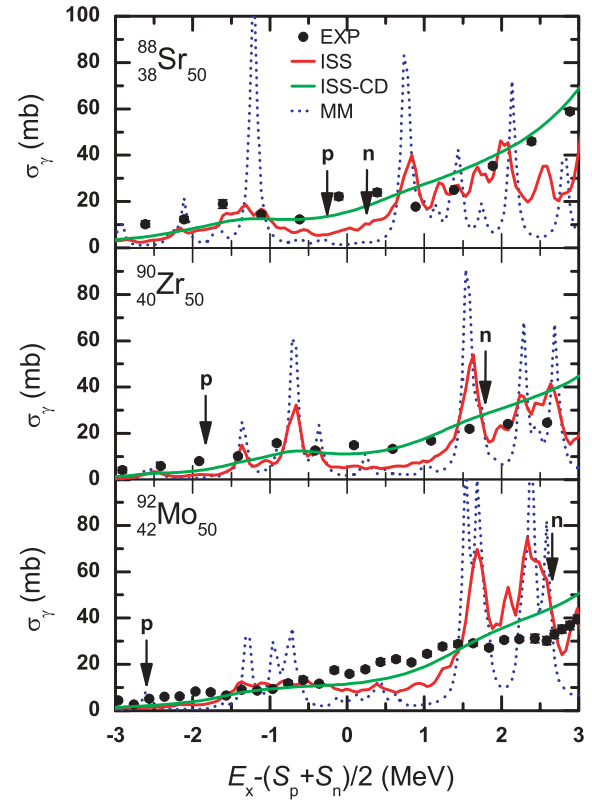

FIG. 4. (Color online) Same as Fig. 3, but the mean of the proton and neutron thresholds are $(S_p + S_n)/2 =$ 10.86, 10.16, 10.06 MeV for $Z =$ 38, 40, 42, respectively. Data from Refs. [17–19].

Figures 3 and 4 zoom into the region near the nucleon emission thresholds. The $M1$ contribution to σ_γ is about 5%, which is consistent with the scarce experimental information [18]. While still fluctuating, σ_γ^{ISS} describes well the experimental strength on the average (cf. Table II). The inclusion of collisional damping in σ_γ^{ISS-CD} levels the fluctuations in the ISS-CD curves, but barely adds any dipole strength. Hence,

TABLE II. Comparison of cumulative cross sections Σ and mean energies $\bar{E}$. Data from Refs. [16,17]. TRK stands for Thomas-Reiche-Kuhn sum rule.

$E1$–$E2$ (MeV)	Σ_{exp} (mb)	Σ_{exp} (% of TRK)	Σ_{ISS-CD} (mb)	Σ_{ISS-CD} (% of TRK)	Σ_{ISS} (mb)	Σ_{MM} (mb)	$\bar{E}_{exp}$ (MeV)	$\bar{E}_{ISS-CD}$ (MeV)	$\bar{E}_{ISS}$ (MeV)	$\bar{E}_{MM}$ (MeV)
^{92}Mo:										
5.1–10.06	30.5 ± 3.8	2.2 ± 0.3	18.6	1.4	21.2	20.1	8.6	8.9	9.0	9.0
9.06–13.06	93.9 ± 6.1	6.9 ± 0.4	93.5	6.8	102.4	85.9	11.4	11.7	11.7	11.6
13.06–20.0	917.8 ± 15.9	67.0 ± 1.2	935.3	68.3	1206.5	1229.2	16.8	16.5	15.9	15.9
^{96}Mo:										
4.3–9.15	23.7 ± 4.5	1.7 ± 0.3	13.9	1.0	11.7	13.0	7.3	8.1	8.4	8.5
8.15–12.15	82.2 ± 8.7	5.8 ± 0.6	80.9	5.7	85.3	69.8	10.7	10.8	10.9	10.8
12.15–20.0	871.4 ± 13.0	61.5 ± 0.9	894.8	63.1	1263.5	1284.6	16.3	16.3	15.8	15.8
^{100}Mo:										
4.3–8.29	20.0 ± 2.7	1.4 ± 0.2	8.6	0.6	5.9	4.7	6.7	7.2	7.2	7.4
7.29–11.29	70.2 ± 10.3	4.8 ± 0.7	73.9	5.0	82.6	56.2	9.8	10.1	10.3	10.0
11.29–20.0	945.8 ± 26.4	64.7 ± 1.8	941.3	64.4	1307.8	1341.8	15.9	15.9	15.7	15.5

the dipole strength near the nucleon emission threshold is determined by the Landau fragmentation of the instantaneous shapes, each of which contributes with its ground state probability. While the resulting dipole strength deviates from a Lorentzian shape, it shows remainders of the underlying particle-hole structure.

Table II shows the cumulative cross sections and averaged energies

$$\Sigma = \int_{E1}^{E2} \sigma(E)\,dE, \quad \bar{E} = \int_{E1}^{E2} E\sigma(E)\,dE / \Sigma. \quad (6)$$

We chose three energy intervals ($E1$–$E2$) for each Mo nuclide: (1) from the energy below which the experimental data are incomplete to the pertinent threshold energies S_n or $(S_n + S_p)/2$ (first row), (2) the astrophysically relevant region from 1 MeV below to 3 MeV above the threshold energies (identical with the intervals in Figs. 3 and 4) (second row), and (3) the GDR region above the second interval extending to 20 MeV (third row). In the astrophysical region, the experiment is very well reproduced by $\Sigma_{\text{ISS}-\text{CD}}$ and $\bar{E}_{\text{ISS}-\text{CD}}$. The Σ_{ISS} are somewhat too large, whereas the Σ_{MM} are too small. For the low-energy region, $\Sigma_{\text{ISS}-\text{CD}}$ underestimates the experiment by a factor of 2. The reason is that the negative parity two-quasiparticle states start at about 5 MeV, which is the minimal energy to excite a particle to the next shell. The repulsive interaction does not shift strength to lower energy. The missing experimental strength should be attributed to negative parity two-phonon excitations, which are not taken into account. Similar agreement of the calculations with experiment is found for the nuclides not included in the table.

In summary, we propose a novel method (ISS-QRPA) for calculating the dipole strength function of nuclei with large-amplitude shape fluctuations, which combines the interacting boson model (IBA) with the quasiparticle random-phase approximation (QRPA). The method is based on the existence of two time scales: the slow shape dynamics and the fast dipole vibrations. Instantaneous-shape sampling (ISS) assumes (i) that the photoabsorption occurs at a fixed shape—described by QRPA—with the probability given by the IBA. We studied the transitional nuclides with ($Z = 38, 40, 42; N = 50$) and ($Z = 42, N = 52, 54, 56, 58$). ISS-QRPA well reproduces the experimental photoabsorption cross sections σ_γ around the nucleon emission threshold, where σ_γ is determined by the Landau fragmentation and the fluctuating shapes. At low energy, the theory underestimates the experimental σ_γ, the cumulative cross section for the region below the threshold being a factor of 2 too low.

[1] http://www-nds.iaea.org/RIPL-2/.

[2] J. Kopecky and M. Uhl, Phys. Rev. C **41**, 1941 (1990).

[3] T. Rauscher and F.-K. Thielemann, At. Data Nucl. Data Tables **75**, 1 (2000).

[4] J. Wambach, Rep. Prog. Phys. **51**, 989 (1988).

[5] V. G. Soloviev, *Theory of Atomic Nuclei: Quasiparticles and Phonons* (Institute of Physics, Bristol, England, 1992).

[6] N. Tsoneva and H. Lenske, J. Phys. G **35**, 014047 (2008).

[7] E. V. Litvinova, P. Ring, and V. Tselyaev, Phys. Rev. C **78**, 014312 (2008).

[8] D. Sarchi *et al.*, Phys. Lett. **B601**, 27 (2004).

[9] F. Dönau *et al.*, Phys. Rev. C **76**, 014317 (2007).

[10] S. Kahane, S. Raman, and J. Dudek, Phys. Rev. C **40**, 2282 (1989).

[11] G. Rusev *et al.*, Phys. Rev. C **73**, 044308 (2006).

[12] F. Iachello and A. Arima, *The Interacting Boson Model* (Cambridge University, Cambridge, England, 1987).

[13] E. A. McCutchan, N. V. Zamfir, and R. F. Casten, Phys. Rev. C **69**, 064306 (2004).

[14] D. Tonev *et al.*, Phys. Rev. C **76**, 044313 (2007).

[15] V. Werner *et al.*, Phys. Rev. C **61**, 021301(R) (2000).

[16] G. Rusev *et al.*, Phys. Rev. C **77**, 064321 (2008).

[17] G. Rusev *et al.*, Phys. Rev. C **79**, 061302(R) (2009).

[18] R. Schwengner *et al.*, Phys. Rev. C **76**, 034321 (2007).

[19] R. Schwengner *et al.*, Phys. Rev. C **78**, 064314 (2008).

[20] http://www.nndc.bnl.gov/ensdf.

[21] P. E. Garrett *et al.*, Phys. Rev. C **68**, 024312 (2003).

[22] G. Cata *et al.*, Z. Phys. A **335**, 271 (1990).

[23] A. Bohr and B. Mottelson, *Nuclear Structure* (W. A. Benjamin, Inc., Reading, Massachusetts, 1975), Vol. II, p. 455ff.